Acupuncture and Herbal Medicine

Effects of electroacupuncture on gut microbiota in a rat model of urticaria

Xianjun Xiao[1], Peiwen Xue[1], Haiyan Qin[2], Di Qin[3], Lu Wang[4], Rongjiang Jin[1], Ying Li[3], Yunzhou Shi[3,*], Juan Li[1,5,*]

[1]School of Health Preservation and Rehabilitation, Chengdu University of Traditional Chinese Medicine, Chengdu, China; [2]Department of Acupuncture, The First Affiliated Hospital of Shenzhen University, Shenzhen, China; [3]Acupuncture and Tuina School, Chengdu University of Traditional Chinese Medicine, Chengdu, China; [4]Department of Acupuncture, Hospital of Chengdu University of Traditional Chinese Medicine, Chengdu, China; [5]Affiliated Sichuan Provincial Rehabilitation Hospital of Chengdu University of TCM, Chengdu, Sichuan, China

Abstract

Objective: Growing evidence suggests a strong link between gut microbiota and the pathogenesis of urticaria, positioning the gut-skin axis as a novel therapeutic target. Despite the efficacy of acupuncture in alleviating urticaria symptoms, the underlying mechanisms remain poorly understood. We investigated the effects of electroacupuncture on gut microbiota in a rat model of urticaria.

Methods: Sprague-Dawley rats were randomly divided into three groups: control, model, and electroacupuncture. An urticaria model was established by combining active systemic and passive cutaneous allergic reactions. Electroacupuncture treatment was administered for 7 days, during which the number of scratches, the diameter of skin sensitization blue spots, and degranulation rate of mast cells were recorded. Inflammation in the sensitized skin was assessed using hematoxylin and eosin staining, and the composition of the gut microbiota was analyzed using 16S rRNA gene sequencing.

Results: Electroacupuncture significantly reduced the frequency of scratching, the diameter of sensitized blue spots, and the degranulation rate of mast cells in rats. The staining results revealed that electroacupuncture decreased inflammatory cell infiltration and fibrous tissue proliferation in the sensitized skin. The 16S rRNA gene sequencing demonstrated that electroacupuncture adjusted the ratio of Firmicutes to Bacteroidetes. Receiver operating characteristic (ROC) curve analysis identified *Parabacteroides johnsonii* as a potential biomarker for diagnosing urticaria (AUC = 0.8516, where AUC stands for the area under the curve) and *Lactobacillus reuteri* and *Limosilactobacillus* as potential biomarkers for predicting the effectiveness of acupuncture treatment (AUC = 0.8281).

Conclusion: Electroacupuncture may alleviate urticaria symptoms by modulating the gut microbiota, providing new theoretical and practical directions for acupuncture treatment of urticaria.

Keywords: Electroacupuncture, Firmicutes/bacteroidetes ratio, Gut microbiota, Gut-skin axis, Urticaria

Graphical abstract: http://links.lww.com/AHM/A166.

Introduction

Urticaria is a common skin disease with a continuously rising annual incidence rate, affecting approximately 20% of the global population[1–2]. It is primarily characterized by wheals, itching, or angioedema[3], which significantly impair patients' quality of life and psychological well-being[2,4]. The pathogenesis of urticaria is complex and is closely related to autoimmune and allergic reactions[5]. Although significant progress has been made in this field in recent years, understanding of its exact mechanisms remains relatively limited. Increasing evidence suggests that changes in the gut microbiota mediated by the gut-skin axis play a critical role in the development of urticaria[6]. Compared with healthy individuals, patients with urticaria show significant differences in the diversity and abundance of their gut microbiota[5,7–8], which potentially contribute to the disease process by triggering pro-inflammatory responses[9]. Animal experiments have demonstrated that alterations in the gut microbiota can promote urticaria[10]. These findings underscore the important role of the gut microbiome in the pathophysiology of urticaria via the gut-skin axis. Therefore, exploring the interactions between gut microbiota and urticaria, along with their underlying mechanisms, is crucial for understanding the fundamental factors of urticaria and developing new therapeutic approaches[11]. Current clinical guidelines aim to fully control the symptoms of urticaria through comprehensive treatment[3]; however, nearly half of the patients respond poorly to first-line treatments such as second-generation

Xianjun Xiao, Peiwen Xue, Haiyan Qin, and Di Qin contributed equally to this work.

**Corresponding author. Yunzhou Shi, E-mail: shiyunzhou@cdutcm.edu.cn; Juan Li, E-mail: 785939016@qq.com.*

Received 31 May 2024 / Accepted 7 February 2025

How to cite this article: *Xiao XJ, Xue PW, Qin HY, Qin D, Wang L, Jin RJ, Li Y, Shi YZ, Li J. Effects of electroacupuncture on gut microbiota in a rat model of urticaria. Acupunct Herb Med 2025;5(1):103–114. DOI: 10.1097/HM9.0000000000000145*

antihistamines[12]. The use of second-line medications, such as omalizumab, is restricted because of their high cost[13–14]. Therefore, there is an urgent need to identify novel and effective treatments[11].

Acupuncture, an ancient traditional alternative therapy, has shown unique advantages in treating urticaria[15]. Our previous clinical studies[16] confirmed that acupuncture can effectively alleviate symptoms such as itching and wheals associated with urticaria. Although the effectiveness of acupuncture has been recognized through clinical evidence, its precise mechanisms of action remain unclear. Recent studies have revealed that electroacupuncture (EA) alleviates urticaria symptoms by affecting the reactive oxygen species (ROS)/transient receptor potential melastatin 2 (TRPM2) signaling pathway, providing key insights into its molecular mechanisms[17]. However, reports on whether acupuncture can modulate gut microbiota through the gut-skin axis to improve urticaria are relatively scarce. We employed a skin allergic reaction method to establish a rat model of urticaria, observe behavioral changes in the rats, and adjust their gut microbiota following acupuncture treatment, with the aim of deepening our understanding of the potential mechanisms by which acupuncture helps in treating urticaria.

Methods

Reagents and chemicals

Ovalbumin (OVA, the protein from chicken egg whites) was sourced from SIGMA Co. (Shanghai, China) (lot number A5503-1G, 1 g). The aluminum hydroxide adjuvant was obtained from InvivoGen Co. (San Diego, CA, USA) (lot number vac-alu-250, 250 mL). Evans Blue Dye was procured from Hefei Bomei Biotechnology Co., Ltd. (Hefei, Anhui, China) (lot number YEO345, 5 g). Isoflurane was obtained from Rayward Co. (Shenzhen, Guangdong, China) (lot number JM20220208, 250 mL). Shandong Qidu Pharmaceutical Co., Ltd. (Zibo, Shandong, China) provided 0.9% NaCl injection (batch number H37020766, 250 mL). Xylene was obtained from Sinopmedicine Group Chemical Reagent Co. Ltd. (Shanghai, China) (lot number 10023418). Anhydrous ethanol was obtained from the same company (batch number 100092683). Toluidine blue dye solution (product number G1032) was obtained from Servicebio Co. (Wuhan, Hubei, China). Hydrochloric acid was acquired from Chengdu Chron Chemicals Co., Ltd. (Chengdu, Sichuan, China) (product number 7647-01-0, 500 mL). Hematoxylin and eosin (HE) stain were provided by Wuhan Servicebio Technology Co., Ltd. (Wuhan, Hubei, China) and Hefei Bomei Biotechnology Co., Ltd., with lot numbers G1004 (500 mL) and YE2080 (25 g), respectively. Neutral gum (lot number BL704A, 100 g) was obtained from Biosharp Biotechnology Co., Ltd. (Hefei, Anhui, China). Finally, paraformaldehyde was sourced from Chengdu Chron Chemicals Co., Ltd. (product number 30525-89-4, 500 mL).

Animals

The study utilized 27 male Sprague-Dawley rats (aged 6 weeks, weighing 150–180 g) purchased from Chengdu Dashuo Experimental Animal Co., Ltd. (Chengdu, Sichuan, China). The animals were maintained in a specific pathogen-free facility with controlled environmental conditions: ambient temperature of (22 ± 2)°C, relative humidity of 40% to 60%, and a standard 12-hour light/dark cycle. The rats received unrestricted access to standard laboratory chow and water. Daily veterinary monitoring was conducted to assess animal welfare and behavior. The animal experiment was performed at the Animal Experimental Center, Chengdu University of Chinese Traditional Medicine (Chengdu, China) and was carried out in strict accordance with the Animal Research: Reporting of In Vivo Experiments (ARRIVE). The animal experiment has been approved by the Animal Ethics Committee of Chengdu University of Traditional Chinese Medicine (Animal use license number: SCXK2020-0030, Animal Ethics Number: 2023-01).

Animal model and treatments

Antiserum preparation

Three rats were administered an antiserum containing OVA (1 mg) and aluminum hydroxide (0.5 mL) in 1 mL of physiological saline solution. This treatment was given on days 1, 3, and 5. After 15 days, blood was drawn *via* abdominal aortic puncture. Blood was centrifuged to separate the antiserum, which was stored in a refrigerator for later use (mixed antisera were selected from three sensitized rats).

Model and treatments

After 1 week of adaptive feeding, the animals were randomly assigned to three groups as follows (n = 8 in each group): i) normal (N) group treated with saline, ii) model (M) group treated with OVA/aluminum hydroxide and saline, and iii) the EA group treated with OVA/aluminum hydroxide and EA. All rats, except those in the normal group, were sensitized by administering an i.h. injection of 1 mL physiological saline solution containing OVA (1 mg) and aluminum hydroxide (0.5 mL) on days 1 and 3. The normal group was administered an i.h. injection of 1 mL normal saline. On day 6, each rat was administered an i.d. injection of 0.2 mL antiserum. Subsequently, antigen attack was i.v. injected with 0.5 mL physiological saline solution containing OVA and 50% Evans Blue (OVA was 1 mg) on day 7, which may cause a rapid allergic reaction due to antigen-antibody binding.

Acupuncture treatment

Sterile acupuncture needles (size: 0.25 mm × 13 mm [diameter: 0.25 mm, length: 13 mm]; manufacturer: Suzhou Acupuncture & Moxibustion Appliance Co., Ltd, Suzhou, P.R. China) and Hans Acupoint Nerve Stimulator (HANS, Beijing, China) were used during the EA treatment. Acupoints were determined according to the experimental acupuncture and the acupuncture point map of the rats. The acupuncture needles were inserted bilaterally at Quchi (LI11) and Tianshu (ST25) to a depth of 13 mm. LI11 is located at the midpoint of the line between the lateral end of the transverse elbow stripe and lateral epicondyle of the humerus. ST25 is

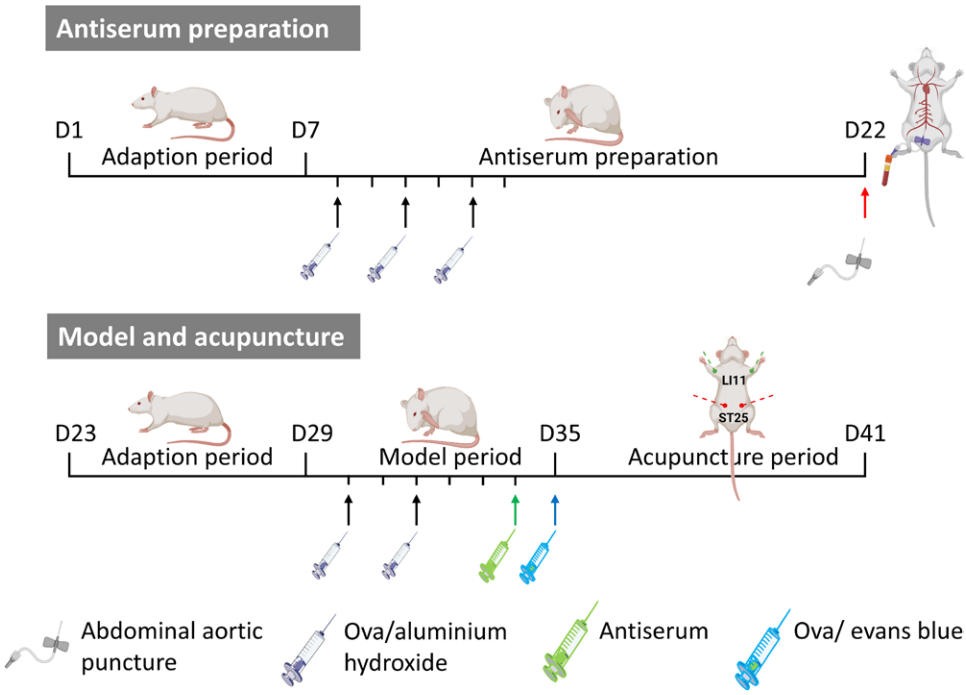

Figure 1. The flowchart of the experiment.

located 2 inches from the center of the umbilicus. EA treatment was performed daily for 7 days. Stimulation waveform selection of dense and sparse waves, stimulation current of 1.5 mA, and frequency of 2/15 Hz for 20 minutes each.

Specimen collection

At the end of acupuncture treatment on day 7, the antigen attack was repeated. Evans: All animals were anesthetized using isoflurane 1 hour after antigen attack. Blood samples were collected by abdominal aortic puncture, dorsal skin tissues were harvested, and approximately 5 g of fresh stool from each rat was collected in a sterile centrifuge tube with a lid. All samples were frozen at –80°C until further studies. A flowchart of the experiment is shown in Figure 1.

Indicator detection

The indications for pruritus included systemic itching behaviors, such as head scratching with the paws, torso scratching with hind claws, and biting at various body parts with the mouth. The frequency of pruritus was recorded for each rat within 30 minutes of sensitization. If the number of scratching incidents was higher in the M group treated with OVA/aluminum hydroxide than in the N group treated with saline, this was considered indicative of successful model establishment.

After the antigen attack, the rats were immediately observed for the appearance of wheals on their backs. The diameter of the blue spot at the site of antiserum injection was measured directly using a ruler on skin extracted from the backs of all rats. For irregular spots, the diameters were calculated as half of the sum of the longest and shortest diameters. The presence of wheals and blue spots with diameters greater than 5 mm on the back skin of the M group, and their absence in the N group, indicated a positive result.

The back skin tissues of the rats were rinsed with a 0.9% sodium chloride solution, fixed with paraformaldehyde, dehydrated, embedded, and sliced. The sections were then dewaxed, stained with hematoxylin, differentiated, subjected to ammonia-reverting blue staining, stained with eosin, subjected to secondary differentiation, another round of ammonia-reverting blue staining, and finally stained with eosin. The observations and image collection were performed using an optical microscope. If the urticaria model exhibited histological features, such as vascular edema, dilation of postcapillary venules, lymphatic vessel expansion in the upper dermis, and varying degrees of mixed inflammatory cell infiltration around the blood vessels, the model was further validated. Histological features were scored on a subjective scale of 0 to 3[18].

Mast cell degranulation in rat skin tissue was assessed using toluidine blue staining. Shaved dorsal skin was fixed overnight in 4% paraformaldehyde at 4°C, followed by paraffin embedding and sectioning at 5-μm thickness. The tissue sections underwent toluidine blue staining (1% solution, 30 minutes, room temperature) and were subsequently differentiated in 0.5% glacial acetic acid for 5 seconds after a brief rinse with distilled water. The sections were then dehydrated using a graded series of alcohols, cleared in xylene, and mounted in neutral gum. Three random visual fields per slide were photographed using a light microscope. The total numbers of mast and degranulated cells were counted and averaged. The mast cell degranulation rate was calculated as follows: (number of degranulated cells/total number of mast cells) × 100.

DNA extraction and 16S rRNA gene sequencing

Total genomic DNA was extracted from stool samples using the TGuide S96 Magnetic Soil/Stool DNA Kit

[Tiangen Biotech (Beijing) Co., Ltd., Beijing, China]. The electrophoresis on a 1.8% agarose gel was employed to assess both the quality and quantity of the extracted DNA. Subsequently, the NanoDrop 2000 UV-Vis spectrophotometer (Thermo Scientific, Wilmington, NC, USA) was utilized to determine the concentration and purity of the DNA. The amplification of the full-length 16S rRNA gene was achieved using the primer set 27F(AGRGTTTGATYNTGGCTCAG) and 1492R(TASGGHTACCTTGTTASGACTT), both of which were appended with sample-specific PacBio barcode sequences facilitate multiplexed sequencing. For polymerase chain reaction (PCR) amplification, the KOD One PCR Master Mix (TOYOBOLife Science, New York, USA) was used, with a protocol consisting of an initial denaturation step at 95°C for 2 minutes, followed by 25 cycles of denaturation at 98°C for 10 seconds, annealing at 55°C for 30 seconds, and extension at 72°C for 1 minute 30 seconds, and a final step at 72°C for 2 minutes. PCR amplicons were purified using VAHTSTM DNA Clean Beads (Vazyme, Nanjing, China) and quantified *via* Qubit 3.0 Fluorometer with dsDNA HS Assay Kit (Invitrogen, Thermo Fisher Scientific, OR, USA). Equal amounts of the quantified amplicons were pooled and processed for SMRTbell library construction using the SMRTbell Express Template Prep Kit 2.0 (Pacific Biosciences, Menlo Park, CA, USA) according to the manufacturer's protocol. The final libraries were sequenced on a PacBio Sequel II platform (Beijing Biomarker Technologies Co., Ltd., Beijing, China) using Sequel II Binding Kit 2.0.

Bioinformatics analysis

Bioinformatics analysis was conducted using BMKCloud (http://www.biocloud.net/). Raw reads from sequencing were filtered and demultiplexed using SMRT Link software (version 8.0), setting minPasses ≥5 and minPredictedAccuracy ≥0.9 to generate circular consensus sequencing (CCS) reads. Lima (version 1.7.0) was used to assign CCS sequences to the respective samples based on their barcodes. CCS reads lacking primers or outside the length range of 1,200 to 1,650 bp were discarded through primer recognition and quality filtering using Cutadapt (version 2.7)[19]. The UCHIME algorithm (version 8.1)[20] was applied to detect and remove the chimeric sequences, yielding clean reads. Sequences with >97% similarity were clustered into operational taxonomic units (OTUs) using USEARCH (version 10.0)[21], discarding OTUs with counts of <2 across all samples. Feature classification of clean reads was performed using DADA2[22] to produce amplicon sequence variants (ASVs), filtering out ASVs with counts less than two in all samples. The taxonomic annotation of the OTUs/ASVs was conducted using the naïve Bayes classifier in QIIME2[23] with the SILVA database (release 138.1)[24], applying a confidence threshold of 70%.

Data analysis and statistical tests

Subsequent analyses were conducted after normalizing the original peak area to the total peak area. The Chao1, ACE, Simpson, and Shannon indices were used to assess alpha diversity. Partial least squares discriminant analysis (PLS-DA) was employed to evaluate the differences in beta diversity among species. Discriminative features were identified using linear discriminant analysis (LDA) effect size (LEfSe), with a logarithmic LDA score of 3.5 set as the threshold. A receiver operating characteristic (ROC) curve was used to explore the potential diagnostic and acupuncture efficacy values of the specific species. Phylogenetic Investigation of Communities by Reconstruction of Unobserved States (PICRUSt2) was used for compositional and differential analyses of Kyoto Encyclopedia of Genes and Genomes (KEGG) metabolic pathways to predict differential functional genes. Continuous variables, such as the diameter of the blue spot and mast cell degranulation rate, are presented as mean ± standard deviation (M ± SD) and percentages (%), respectively. The Wilcoxon rank-sum test was used for numerical variables that did not conform to a normal distribution, whereas one-way analysis of variance (ANOVA) was used for variables that conformed. Scratch numbers were analyzed using repeated-measures ANOVA. Statistical significance was set at a P value <0.05 (two-sided) and was accepted as the cutoff for statistical significance. Statistical analyses were performed using SPSS 25.0, R and GraphPad Prism software.

Results

Assessment of scratching behavior

The results showed that the number of scratched rats varied with time ($P < 0.05$), and the difference between the groups was significant ($P < 0.05$). There was no difference in scratching among the three groups at the baseline period ($P > 0.05$). During the modeling period, the number of scratches in group M was significantly higher than that in group N ($P < 0.05$) but did not differ from that in the group EA ($P > 0.05$). During the acupuncture period, the number of scratches in the EA group was significantly lower than that in the M group ($P < 0.05$), and there was no difference compared to the N group ($P > 0.05$) (Figure 2).

Wheals and diameter in blue plaque

No significant sensitizing wheals or blue spots were observed in the dorsal dehairing areas of rats in the N group. Compared to the N group, obvious wheals and sensitized blue spots were observed in the M group, and the diameter of the blue spots was >5 mm ($P < 0.01$). Compared to the M group, the diameter of the sensitized blue spots in the EA group was significantly reduced ($P < 0.01$) (Figure 3).

HE staining

As shown in Figure 4, following HE staining, compared to the N group, obvious localized degeneration and necrosis of collagen fibers in the dermis with blurred margins, infiltration of inflammatory cells such as neutrophils and lymphocytes, and a small amount of fibrous tissue hyperplasia were observed in rats of M group ($P < 0.01$). In addition, EA treatment inhibited inflammatory cell infiltration compared to group M, and the apparent proliferation of fibrous tissue was not evident ($P < 0.05$).

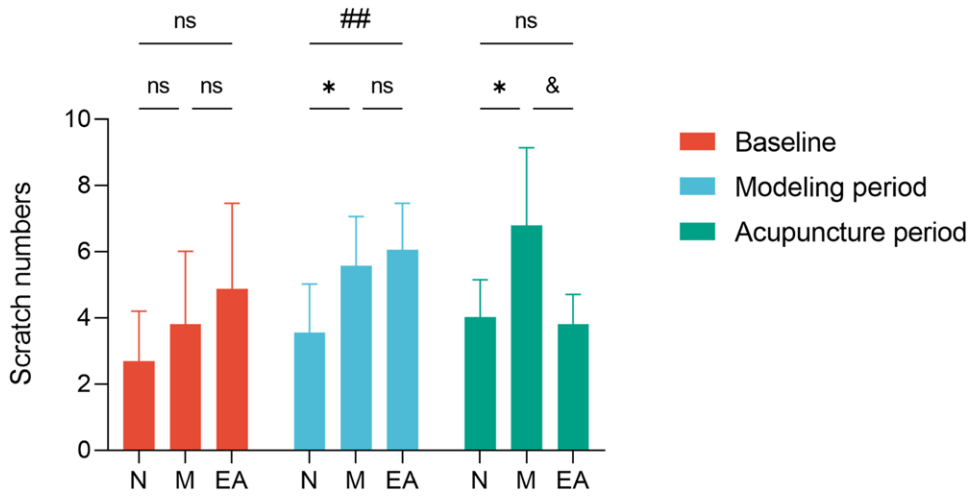

Figure 2. Change of scratching numbers (*$P < 0.05$ *vs*. group N, $^{\&}P < 0.05$ *vs*. group M, $^{\#\#}P < 0.01$ *vs*. EA group). EA: Electroacupuncture; M: Model; N: Normal; ns: No significant.

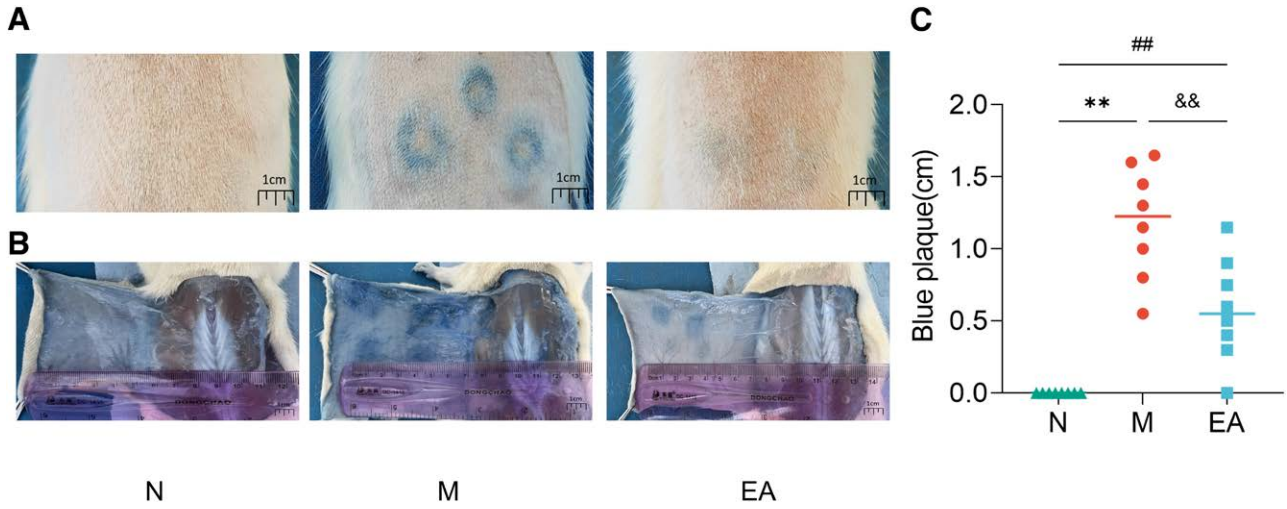

Figure 3. Wheals and diameter in blue plaque. (A) Wheals in dorsal dehairing area. (B) Blue spot in dorsal dehairing area. (C) Statistic analysis of blue spot. **$P < 0.01$ *vs*. group N, $^{\&\&}P < 0.01$ *vs*. group M, $^{\#\#}P < 0.01$ *vs*. EA group. EA: Electroacupuncture; M: Model; N: Normal.

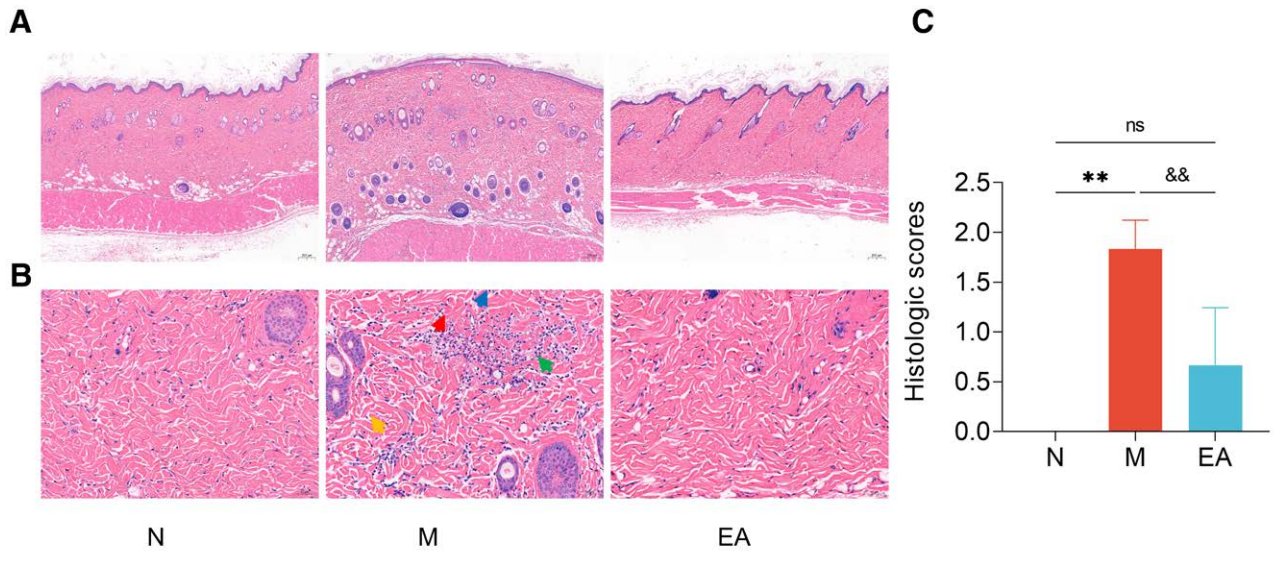

Figure 4. HE staining of dorsal skin at high and low magnification. (A) ×40, (B) ×200, (C) Histologic scores. ↑: Necrotic collagen fibers, ↑: neutrophils, ↑: lymphocytes, ↑: fibroblasts. **$P < 0.01$ *vs*. group N, $^{\&\&}P < 0.01$ *vs*. group M. EA: Electroacupuncture; HE: Hematoxylin and eosin; M: Model; N: Normal; ns: No significant.

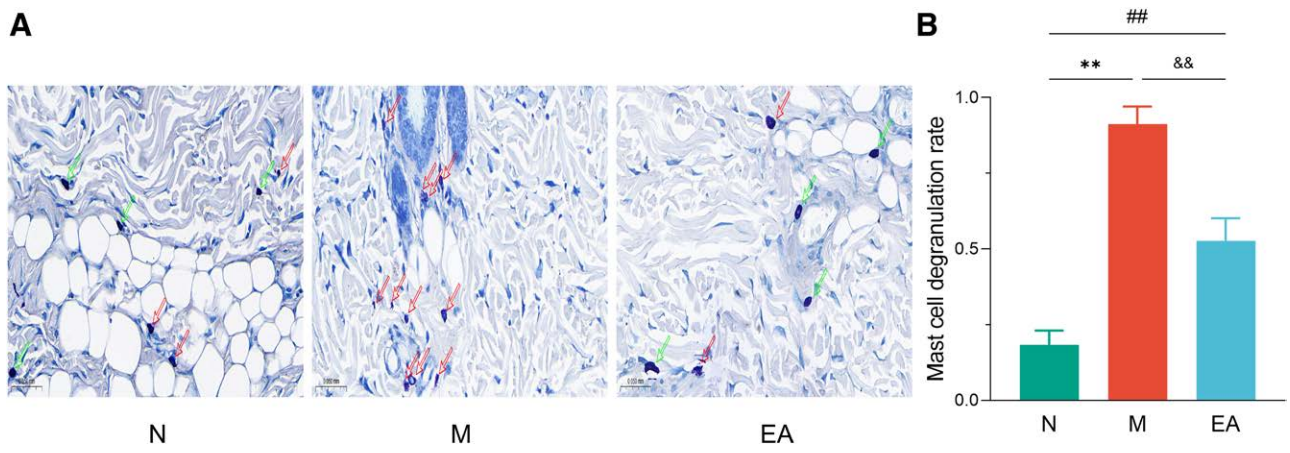

Figure 5. The results of toluidine blue staining. (A) Toluidine blue staining of dorsal skin,×400. (B) Change of mast cell degranulation rate. ↑: Mast cell degranulation, ↑: mast cell, $^{**}P < 0.01$ *vs*. group N, $^{\&\&}P < 0.01$ *vs*. group M, $^{\#\#}P < 0.01$ *vs*. EA group. EA: Electroacupuncture; M: Model; N: Normal.

Toluidine blue staining

Mast cells from all three groups were stained dark purple. Most of the cell membranes of the mast cells in the N group were smooth and complete, with clear nuclei. In the M group, most of the mast cell cytomembranes were ruptured and incomplete, with varying numbers of heterostained granules scattered around the cells. Compared to the N group, the rate of degranulation was significantly higher in the M group ($P < 0.01$). Compared with the M group, the degranulation rate in the EA group was significantly decreased ($P < 0.01$) (Figure 5).

Diversities of gut microbiota

A total of 2,259,713 high-quality sequences (average 94,155) and 524 OTUs were obtained from the 24 fecal samples. Rarefaction, Shannon index, rank abundance, and species cumulative curves [Supplementary Figures S1–S4, http://links.lww.com/AHM/A159] indicated adequate sample size, species saturation, and a high degree of homogeneity for subsequent analyses. Significant differences were detected in the alpha diversity between the N and M groups for the Simpson and Shannon indices (Figure 6A). There were no statistically significant differences in the other intergroup comparisons or indices. In the PLS-DA plots, the samples from the three groups were clustered within groups and separated between groups (Figure 6B). The difference in beta diversity was significant in the N, M, and EA groups according to permanova ($R^2 = 0.15$, $P = 0.014$) and Adosim ($R = 0.14$, $P = 0.023$) analyses.

The abundance of gut microbiota

When comparing the abundance of microbiota, we found that the three groups of gut microbiota were mainly composed of Firmicutes and Bacteroidetes. At the phylum level, *Firmicutes* and *Bacteroidetes* were dominant in all three groups (Figure 7A and Supplementary Table S1, http://links.lww.com/AHM/A160). The relative abundance of Firmicutes was N > EA > M, while the relative abundance of *Bacteroidetes* was N < EA < M. Therefore, the *Firmicutes/Bacteroidetes* (F/B) was N > EA > M. At the genus level, we observed an increase in the relative abundance of *unclassified_Muribaculaceae*, *Limosilactobacillus*, *Lactobacillus*, *unclassified_Prevotellaceae*,*unclassified_Clostridia_UCG_014*, and *CAG_873* in group M compared to group N, whereas the relative abundance of *Ligilactobacillus*, *Muribaculum*, *Alloprevotella*, and *Lachnospiraceae_NK4A136_group* was decreased in group M compared with N. What's more, the relative abundance of *unclassified_Muribaculaceae*, *Limosilactobacillus*, *Lactobacillus*, *unclassified_Clostridia_UCG_014*, and *Muribaculum* was increased in EA, whereas the relative abundance of *Ligilactobacillus*, *unclassified_Prevotellaceae*, *Alloprevotella*, *CAG_873*, and *Lachnospiraceae_NK4A136_group* was decreased in this group compared with M (Figure 7B, Supplementary Table S2, http://links.lww.com/AHM/A161).

Differences analysis of gut microbiota

Differential microbiota were identified using LEfSe (LDA score >3.5, $P < 0.05$). As shown in the LDA bar plot, *g_Ligilactobacillus*, *s_Ligilactobacillus murinus*, *g_Lachnoclostridium*, and *s_Bacteroides caecimuris* were significantly enriched in group N, *s_unclassified_Lachnospiraceae_NK4A136_group*, *o_onoglobales*, *f_Monoglobaceae*, *g_Monoglobu*, and *s_Parabaeteroides johnsonii* were significantly enriched in group M, and *g_Lirosilactobacillus* and *s_Lactobacillus reuteri* were significantly enriched in group EA (Figure 8).

Candidate markers by ROC curve

To explore whether the above differential microbiota could serve as potential biomarkers for diagnosing urticaria and predicting the efficacy of acupuncture, we used the relative abundance of the differential microbiota screened by the left analysis as a predictor. The area under the ROC curve (AUC) was used to evaluate the accuracy of potential biomarkers. When diagnosing urticaria, ROC analysis showed that the AUC values of *s_Parabacteroides_johnsonii* was 0.8516 (95% confidence interval [CI], 0.64–1.00, $P = 0.018$) and its cutoff value was 4.5. When predicting the efficacy of

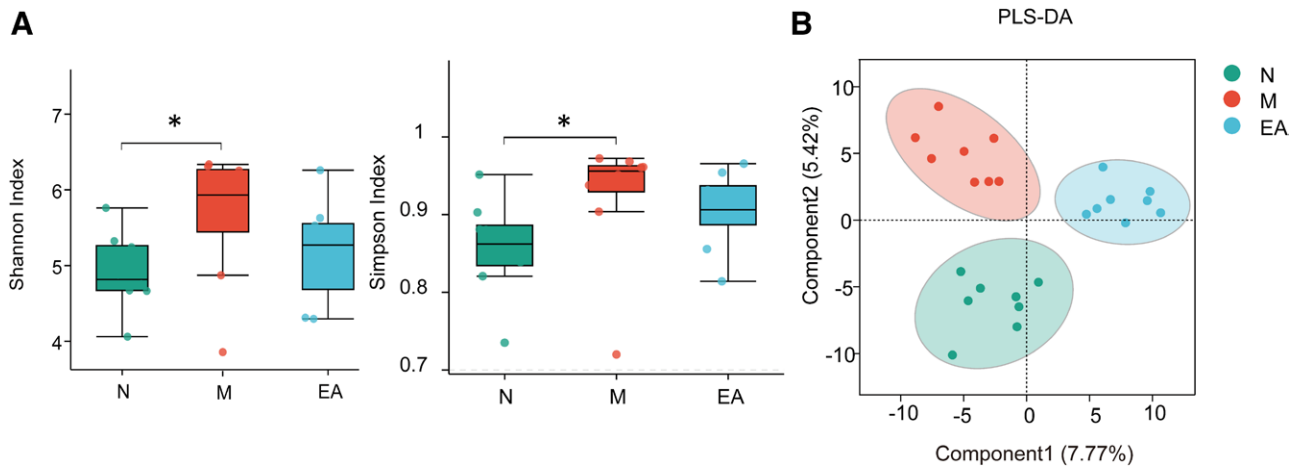

Figure 6. Diversities of gut microbiota. (A) Alpha diversity measured using the Shannon and Simpson indices. (B) Beta diversity measured using PLS-DA, *$P < 0.05$ *vs*. group M. EA: Electroacupuncture; M: Model; N: Normal; PLS-DA: Partial least squares discriminant analysis.

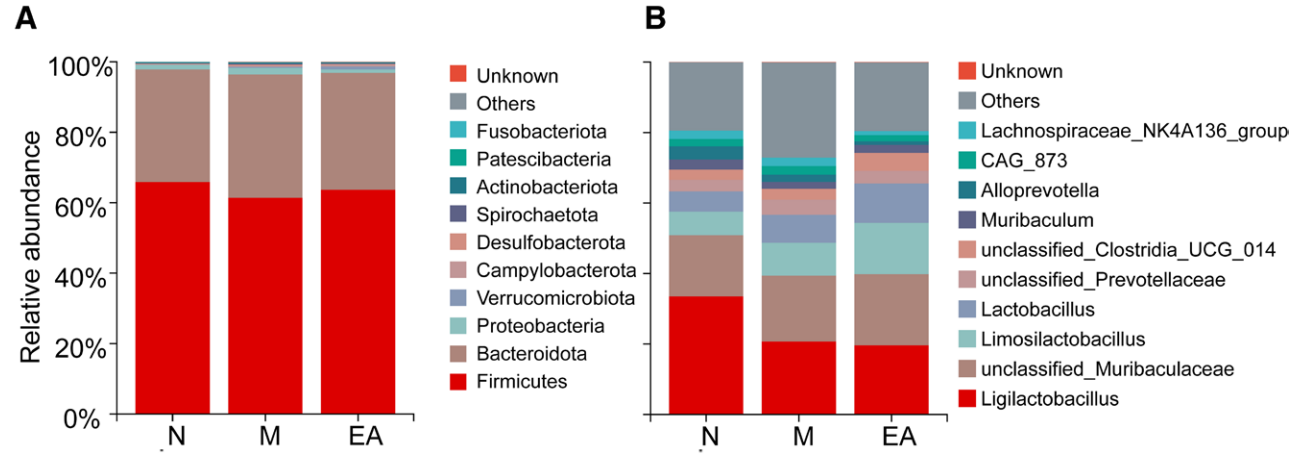

Figure 7. The relative abundance at phylum level (A) and genus level (B). EA: Electroacupuncture; M: Model; N: Normal.

acupuncture, ROC analysis showed that the AUC values of both *L. reuteri* and *Limosilactobacillus* were 0.8281 (95% CI, 0.617–1.00, $P = 0.027$). The cutoff values for these microbiota were 5,540 and 5,542.5, respectively (Figure 9).

Predicted metabolic functions

Differential analysis of the KEGG metabolic pathways showed that at the class 3 level, there were differences in 12 metabolic pathways between groups M and N. In group M, more microbes were enriched in GABAergic synapses, glutamatergic synapses, proximal renal tubular bicarbonate recycling, butyrate metabolism, microRNAs in cancer and proteasome metabolic pathways, β-lactam resistance, RNA degradation, vancomycin resistance, penicillin and cephalosporin biosynthesis, starch and sucrose metabolism, and atrazine degradation microbial enrichment decreased (Figure 10A and Supplementary Table S3, http://links.lww.com/AHM/A162). The EA group differed from the M group in 15 metabolic pathways. After EA intervention, pyruvate metabolism, central carbon metabolism in cancer, type I diabetes mellitus, synthesis and degradation of ketone bodies, D-glutamine and D-glutamate metabolism, nonribosomal peptide structures, pentose phosphate pathway, renal cell carcinoma, glucagon signaling pathway, biosynthesis of vancomycin group antibiotics, and propanoate metabolism pathway were significantly elevated, while stilbenoid, diarylheptanoid and gingerol biosynthesis, longevity regulating pathway-multiple species, biosynthesis of unsaturated fatty acids microorganisms, and Salmonella infection pathways significantly decreased (Figure 10B and Supplementary Table S4, http://links.lww.com/AHM/A163).

Discussion

The concept of the "gut-skin axis" emphasizes the close connection between the gut microbiota and urticaria, opening potential new avenues for treatment[25–26]. Although the gut microbiota has been considered a key factor in the pathogenesis of urticaria[8,27], research on how acupuncture can regulate these microbial communities to treat urticaria remains insufficient. In this study, we simulated urticaria through systemic active immunity and passive cutaneous allergic reactions, and observed significant gut microbiota dysbiosis in rats, supporting the role of the gut-skin axis in urticaria pathogenesis. Furthermore, EA intervention not only significantly alleviated the symptoms of urticaria in the model rats but

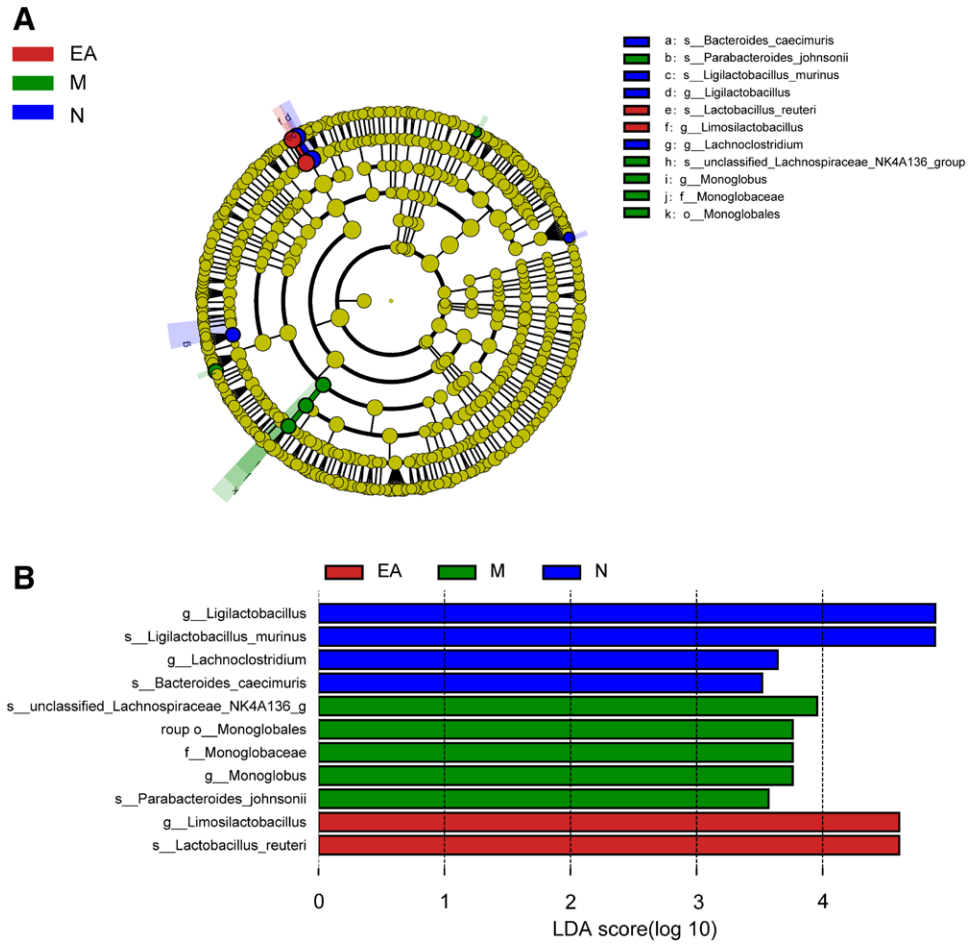

Figure 8. Potential diagnostic markers obtained by LDA. EA: Electroacupuncture; LDA: Linear discriminant analysis; M: Model; N: Normal.

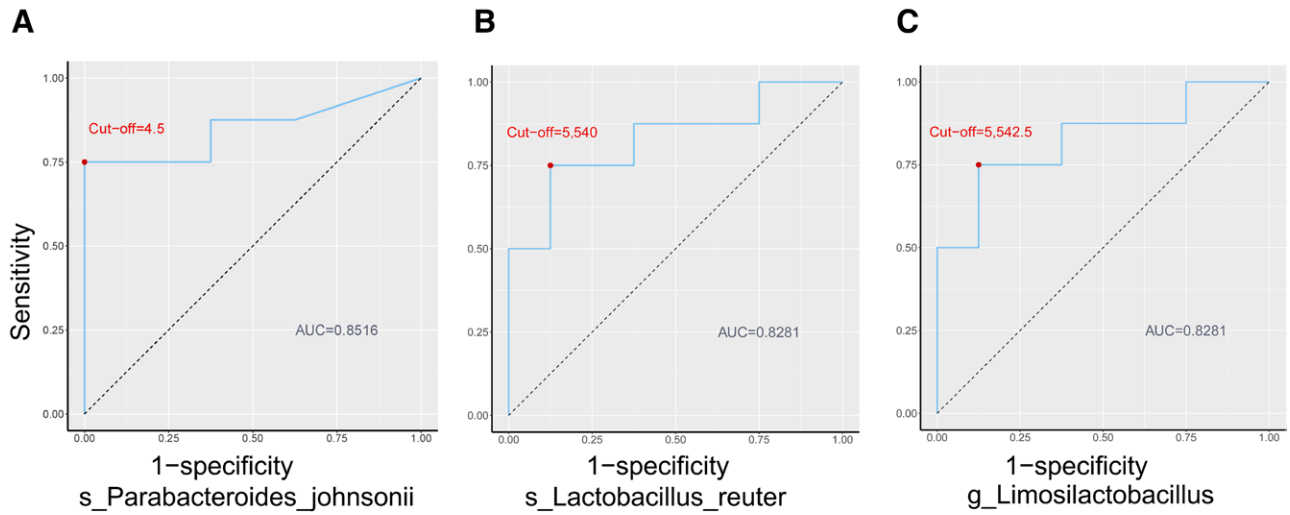

Figure 9. ROC analysis based on the relative abundance for potential biomarkers. (A) Group M for diagnosing urticaria. (B) and (C) Group EA for predicting efficacy. AUC: Area under the curve; EA: Electroacupuncture; M: Model; ROC: Receiver operating characteristics.

also improved the abnormalities in the gut microbiota, further revealing the potential mechanism by which acupuncture may treat urticaria through the regulation of the gut microbiota.

Our previous clinical studies confirmed that acupuncture effectively alleviated the symptoms of itching and wheals associated with urticaria[16]. This study further demonstrated that EA can effectively reduce the frequency of scratching, the diameter of sensitized blue spots, and the degranulation rate of mast cells in rats with urticaria. This is consistent with previous findings[17], and further confirms the potential efficacy of EA in modulating urticaria.

Recent studies have emphasized that disruptions in the gut microbiota and their associated metabolic products are important regulators of urticaria[26]. Recent

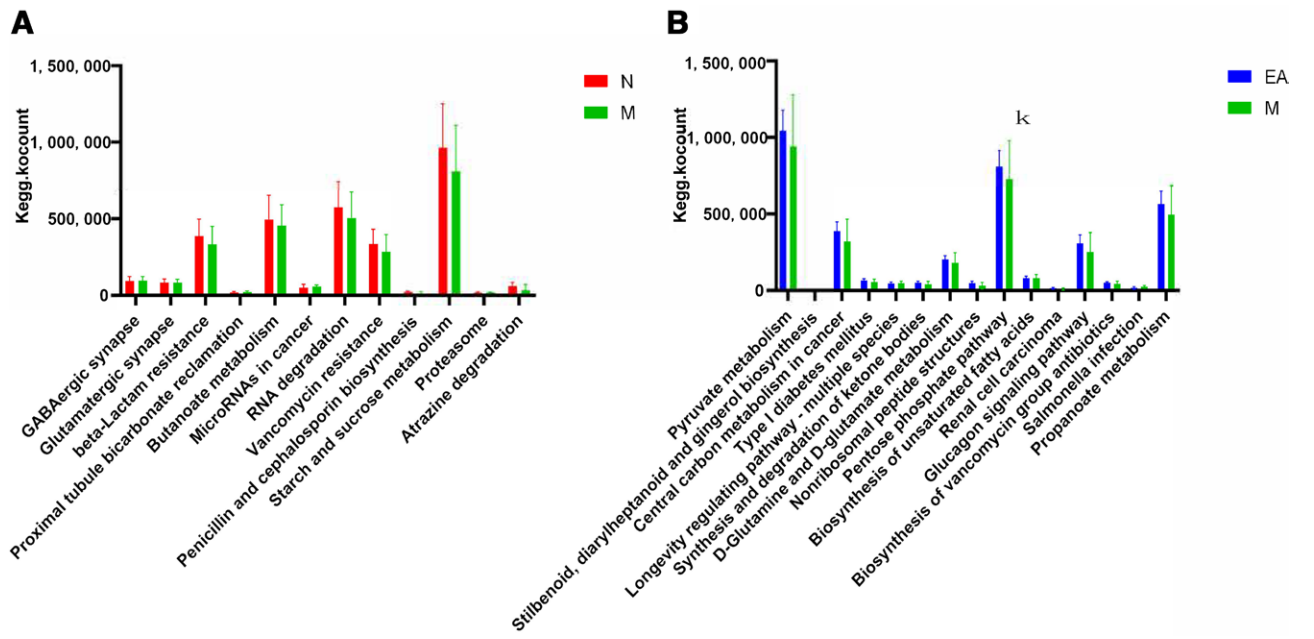

Figure 10. Predicted metabolic functions analysis. (A) Group N *vs*. group M, (B) group M *vs*. group EA. EA: Electroacupuncture; M: Model; N: Normal.

Mendelian randomization studies confirmed a bidirectional causal relationship between the gut microbiota and urticaria[28]. In this study, changes in urticaria induced by skin sensitization led to dysbiosis at various levels in the rat gut microbiome, providing new evidence for an interactive relationship between the gut microbiota and urticaria. *Firmicutes* and *Bacteroidetes* dominate the human gut microbiome and account for more than 90% of the total microbiota[29]. A decrease in the F/B ratio is commonly considered a diagnostic sign of gut microbiota disorder[30]. In this study, the F/B ratio in the model group was significantly lower than that in the normal group. However, after EA intervention, the F/B ratio significantly increased and approached the level of the normal group, indicating the potential of EA to correct gut microbiota disorders. Building on current research linking microbiota abundance and microbial metabolites to the clinical symptoms and pathogenesis of urticaria, our findings further suggest that EA may effectively treat urticaria by modulating the gut microbiota. This modulation may have far-reaching implications beyond those of urticaria. For instance, restoration of the microbial balance may influence systemic inflammation, immune function, and even neurological processes, given the wide-ranging effects of the gut microbiome on human health. Future research should explore whether microbial changes induced by acupuncture lead to alterations in microbial metabolites, such as short-chain fatty acids, which are known to have immunomodulatory effects[26].

In terms of microbial abundance, our study revealed an interesting phenomenon in which the abundance of *Muribaculaceae*, *Lactobacillus*, and *Clostridia* in the model group was higher than that in the normal group and even higher in the EA group. This contrasts sharply with previous clinical studies[7,27,31] that found that these microbial groups were less abundant in patients with chronic urticarial (CU) compared to healthy individuals. This difference may be due to our data reflecting the emergency response of acute urticaria model rats, whereas clinical data were obtained from patients with CU. This suggests a potential biphasic response of the gut microbiome to urticaria, with an initial protective increase in certain bacteria during the acute phase, followed by their depletion in chronic conditions. This suggests that at different stages of disease, the gut microbiota may undergo adaptive changes or compensatory responses to restore balance, highlighting the complexity and dynamics of the gut microbiome. Additionally, existing research[27] indicates that *Lactobacillus* has a protective effect against urticaria. Our finding that EA can increase the abundance of *Lactobacillus* supports the possibility that this treatment could help restore the healthy state of the gut microbiota and positively modulate urticaria. Future research should aim to elucidate the specific mechanisms by which acupuncture influences microbial populations and investigate the functional consequences of these microbial shifts in relation to urticaria symptoms.

To delve deeper into the microbiological characteristics of urticaria, this study employed LEfSe analysis to identify microbial groups that were significantly associated with the diagnosis and treatment of urticaria. The analysis revealed a significant difference between *Parabacteroides johnsonii* in the normal group and the model group (AUC = 0.85, $P = 0.018$), suggesting its potential moderate diagnostic value. *Parabacteroides johnsonii* is a Gram-negative, anaerobic, non-spore-forming, rod-shaped bacterium[32]. Clinical studies have shown its increased abundance in certain immune-mediated conditions[33], and its ability to induce interferon-γ producing CD8 T cells in the intestine[34], suggesting a potential role in urticaria pathogenesis. Additionally, our analysis found significant differences between *L. reuteri* (AUC = 0.83, $P = 0.027$) and *Limosilactobacillus* (AUC = 0.83, $P = 0.027$) in the EA group compared to the model group, supporting

the moderate predictive value of these strains for the effectiveness of EA treatment for urticaria. *L. reuteri* is known to have multiple positive effects on host health and the immune system[35], including the induction of anti-inflammatory regulatory T cells (Tregs)[36] and reduction of pro-inflammatory cytokines[37–38]. It can also suppress intestinal inflammation and regulate gut microbiota[39], thereby promoting the gut ecological balance. *Limosilactobacillus* is an important member of the genus *Lactobacillus*[40] and exhibits significant immunomodulatory effects. It boosts anti-inflammatory cytokines and significantly lowers pro-inflammatory tumor necrosis factor-alpha (TNF-α) levels[41–43], which is crucial in managing urticaria-related inflammation[44]. Furthermore, *Limosilactobacillus* improves the diversity and abundance of the gut microbiota, primarily by increasing beneficial bacteria[45–46] and reducing harmful bacteria[47–48], thus promoting the gut ecosystem balance. *Limosilactobacillus* also enhances the skin barrier function by modulating skin protein expression[49]. It can also modulate Th1/Th2 cytokines balance, promote Tregs, and reduce IgE production, thereby alleviating dermatitis symptoms in mouse models[50–51]. While Treg numbers and functionality are often reduced in patients with CU[52–53], the influence of *Limosilactobacillus* on the Th1/Th2 balance and Treg promotion hints at its potential to help manage urticaria. Furthermore, *L. reuteri* was originally part of the traditional *Lactobacillus* genus[54]. In clinical studies, the abundance of *Lactobacillus* in patients with urticaria is significantly lower than that in healthy subjects[7,27], suggesting that *Lactobacillus* may play a protective role against the occurrence of urticaria. This aligns with our finding that the abundance of *Lactobacillus* may be a key factor influencing the treatment outcomes of urticaria.

The discovery that acupuncture can improve urticaria by modulating the gut microbiome opens new avenues for future clinical applications. Integrating acupuncture with conventional pharmacological treatments can lead to personalized therapeutic strategies. For instance, patient gut microbiome profiles could potentially be used to predict the efficacy of acupuncture treatment, thereby optimizing treatment protocols. Moreover, the ability of acupuncture to modulate the gut microbiome may reduce the required dosage of conventional medications, a potential advantage that warrants further investigation in clinical trials. Given our observations on the regulatory effects of acupuncture on the gut microbiome, we recommend the incorporation of gut health interventions into the comprehensive management of urticaria. This could include dietary guidance and probiotic supplementation to complement acupuncture treatment, potentially enhancing overall therapeutic outcomes.

Our study provides novel insights into the treatment of urticaria. Future studies should focus on elucidating the specific mechanisms by which acupuncture modulates the gut microbiome, and how these findings can be translated into more effective clinical intervention strategies. This approach not only offers new perspectives on treating urticaria but also paves the way for more holistic and personalized treatment regimens in dermatology.

This study has two main limitations. First, we did not obtain sufficient data to clearly define the relationship between the biological markers of urticaria and changes in the gut microbiome. This limits our understanding of the role of the gut microbiota in the pathogenesis of urticaria and the impact of acupuncture on this process. Furthermore, additional studies are needed, such as those involving fecal microbiota transplantation, to investigate the specific effects of acupuncture on the regulation of the gut microbiota and its metabolic products in rat models of urticaria. Therefore, to validate the effectiveness of acupuncture and explore its underlying mechanisms, future studies should employ a broader range of clinical and experimental approaches. This includes the use of advanced sequencing technologies such as metagenomics to thoroughly analyze how acupuncture affects the gut microbiota and its functions in patients with urticaria.

Conclusion

In summary, these results support the hypothesis that acupuncture can effectively treat urticaria by restoring the balance of the gut microbiota. Additionally, this study highlights the close interaction between the gut and skin, providing new insights into the potential mechanisms of acupuncture in the treatment of urticaria.

Conflict of interest statement

The authors declare no conflict of interest.

Funding

This study was supported by grants from the National Natural Science Foundation of China (82205283), the Natural Science Foundation of Sichuan Provincial Department of Science and Technology (24NSFSC1549), the China Postdoctoral Science Foundation (2022MD723719), and Chengdu University of Traditional Chinese Medicine's 2024 Undergraduate Innovation and Entrepreneurship Training Program Project (202410633015).

Author contributions

Xianjun Xiao, Rongjiang Jin, and Ying Li conceived and designed the experiments; Xianjun Xiao, Peiwen Xue, Haiyan Qin, Di Qin, and Lu Wang conducted the experiments; Xianjun Xiao, Yunzhou Shi, and Juan Li analyzed the data and wrote the manuscript. All authors reviewed the manuscript and agreed to the final version for submission.

Ethical approval of studies and informed consent

The animal experiment has been approved by the Animal Ethics Committee of Chengdu University of Traditional Chinese Medicine (Animal use license number: SCXK2020-0030, Animal Ethics Number: 2023-01).

Acknowledgments

None.

Data availability

The datasets generated and/or analyzed during the current study are available from the corresponding author on reasonable request. Additional information and supporting data can be found in the Supplementary Materials section of this article.

References

[1] Kolkhir P, Gimenez-Arnau AM, Kulthanan K, et al. Urticaria. *Nat Rev Dis Primers* 2022;8(1):61. doi:10.1038/s41572-022-00389-z.

[2] Goncalo M, Gimenez-Arnau A, Al-Ahmad M, et al. The global burden of chronic urticaria for the patient and society. *Br J Dermatol* 2021;184(2):226–236. doi:10.1111/bjd.19561.

[3] Zuberbier T, Abdul Latiff AH, Abuzakouk M, et al. The international EAACI/GA(2)LEN/EuroGuiDerm/APAAACI guideline for the definition, classification, diagnosis, and management of urticaria. *Allergy* 2022;77(3):734–766. doi:10.1111/all.15090.

[4] Tawil S, Irani C, Kfoury R, et al. Association of chronic urticaria with psychological distress: a multicentre cross-sectional study. *Acta Derm Venereol* 2023;103:adv00865. doi:10.2340/actadv.v102.2939.

[5] Zhang X, Zhang J, Chu Z, et al. Gut microbiome alterations and functional prediction in chronic spontaneous urticaria patients. *J Microbiol Biotechnol* 2021;31(5):747–755. doi:10.4014/jmb.2012.12022.

[6] Kristo M, Lugovic-Mihic L, Munoz M, et al. Gut microbiome composition in patients with chronic urticaria: a review of current evidence and data. *Life (Basel)* 2023;13(1):152. doi:10.3390/life13010152.

[7] Wang D, Guo S, He H, et al. Gut microbiome and serum metabolome analyses identify unsaturated fatty acids and butanoate metabolism induced by gut microbiota in patients with chronic spontaneous urticaria. *Front Cell Infect Microbiol* 2020;10:24. doi:10.3389/fcimb.2020.00024.

[8] Wang X, Yi W, He L, et al. Abnormalities in gut microbiota and metabolism in patients with chronic spontaneous urticaria. *Front Immunol* 2021;12:691304. doi:10.3389/fimmu.2021.691304.

[9] Al Bander Z, Nitert MD, Mousa A, et al. The gut microbiota and inflammation: an overview. *Int J Environ Res Public Health* 2020;17(20):7618. doi:10.3390/ijerph17207618.

[10] Zhu L, Jian X, Zhou B, et al. Gut microbiota facilitate chronic spontaneous urticaria. *Nat Commun* 2024;15(1):112. doi:10.1038/s41467-023-44373-x.

[11] Amin P, Levin L, Holmes SJ, et al. Investigation of patient-specific characteristics associated with treatment outcomes for chronic urticaria. *J Allergy Clin Immunol Pract* 2015;3(3):400–407. doi:10.1016/j.jaip.2014.12.007.

[12] Guillen-Aguinaga S, Jauregui Presa I, Aguinaga-Ontoso E, et al. Updosing nonsedating antihistamines in patients with chronic spontaneous urticaria: a systematic review and meta-analysis. *Br J Dermatol* 2016;175(6):1153–1165. doi:10.1111/bjd.14768.

[13] Kanters TA, Thio HB, Hakkaart L. Cost-effectiveness of omalizumab for the treatment of chronic spontaneous urticaria. *Br J Dermatol* 2018;179(3):702–708. doi:10.1111/bjd.16476.

[14] Türk M, Yılmaz I, Şahiner M, et al. Experience-based advice on stepping up and stepping down the therapeutic management of chronic spontaneous urticaria: Where is the guidance? *Allergy* 2022;77(5):1626–1630. doi:10.1111/all.15227.

[15] Liang Y, Chen X, Ma B. Literature analysis of acupuncture for urticaria from Encyclopaedia of Traditional Chinese Medicine. *Int J Trad Chin Med*. 2019;41(5):506–509. doi:10.3760/cma.j.issn.1673-4246.2019.05.016.

[16] Zheng H, Xiao XJ, Shi YZ, et al. Efficacy of acupuncture for chronic spontaneous urticaria: a randomized controlled trial. *Ann Intern Med* 2023;176(12):1617–1624. doi:10.7326/M23-1043.

[17] Li JQ, Li SJ, Wang L, et al. Electroacupuncture preconditioning relieves cutaneous passive anaphylaxis by down-regulating IP3 mediated ROS/TRPM2 signaling pathway and inhibiting mast cell degranulation in rats with urticaria. *Zhen Ci Yan Jiu* 2023;48(3):274–280. doi:10.13702/j.1000-0607.20220166.

[18] Peng L, Wen L, Zhang J, et al. Circadian pharmacological effects of paeoniflorin on mice with urticaria-like lesions. *Front Pharmacol* 2021;12:639580. doi:10.3389/fphar.2021.639580.

[19] Bolger AM, Lohse M, Usadel B. Trimmomatic: a flexible trimmer for Illumina sequence data. *Bioinformatics* 2014;30(15):2114–2120. doi:10.1093/bioinformatics/btu170.

[20] Edgar RC, Haas BJ, Clemente JC, et al. UCHIME improves sensitivity and speed of chimera detection. *Bioinformatics* 2011;27(16):2194–2200. doi:10.1093/bioinformatics/btr381.

[21] Edgar RC. UPARSE: highly accurate OTU sequences from microbial amplicon reads. *Nat Methods* 2013;10(10):996–998. doi:10.1038/nmeth.2604.

[22] Callahan BJ, McMurdie PJ, Rosen MJ, et al. DADA2: High-resolution sample inference from Illumina amplicon data. *Nat Methods* 2016;13(7):581–583. doi:10.1038/nmeth.3869.

[23] Bolyen E, Rideout JR, Dillon MR, et al. Reproducible, interactive, scalable and extensible microbiome data science using QIIME 2. *Nat Biotechnol* 2019;37(8):852–857. doi:10.1038/s41587-019-0209-9.

[24] Quast C, Pruesse E, Yilmaz P, et al. The SILVA ribosomal RNA gene database project: improved data processing and web-based tools. *Nucleic Acids Res* 2013;41(Database issue):D590–D596. doi:10.1093/nar/gks1219.

[25] Mahmud MR, Akter S, Tamanna SK, et al. Impact of gut microbiome on skin health: gut-skin axis observed through the lenses of therapeutics and skin diseases. *Gut Microbes* 2022;14(1):2096995. doi:10.1080/19490976.2022.2096995.

[26] Xiao X, Hu X, Yao J, et al. The role of short-chain fatty acids in inflammatory skin diseases. *Front Microbiol* 2022;13:1083432. doi:10.3389/fmicb.2022.1083432.

[27] Rezazadeh A, Shahabi S, Bagheri M, et al. The protective effect of Lactobacillus and Bifidobacterium as the gut microbiota members against chronic urticaria. *Int Immunopharmacol* 2018;59:168–173. doi:10.1016/j.intimp.2018.04.007.

[28] Shi YZ, Tao QF, Qin HY, et al. Causal relationship between gut microbiota and urticaria: a bidirectional two-sample Mendelian randomization study. *Front Microbiol* 2023;14:1189484. doi:10.3389/fmicb.2023.1189484.

[29] Eckburg PB, Bik EM, Bernstein CN, et al. Diversity of the human intestinal microbial flora. *Science* 2005;308(5728):1635–1638. doi:10.1126/science.1110591.

[30] Burrello C, Garavaglia F, Cribiù FM, et al. Therapeutic faecal microbiota transplantation controls intestinal inflammation through IL10 secretion by immune cells. *Nat Commun* 2018;9(1):5184. doi:10.1038/s41467-018-07359-8.

[31] Liu R, Peng C, Jing D, et al. Biomarkers of gut microbiota in chronic spontaneous urticaria and symptomatic dermographism. *Front Cell Infect Microbiol* 2021;11:703126. doi:10.3389/fcimb.2021.703126.

[32] Cui Y, Zhang L, Wang X, et al. Roles of intestinal parabacteroides in human health and diseases. *FEMS Microbiol Lett* 2022;369(1):fnac072. doi:10.1093/femsle/fnac072.

[33] Moreno-Arrones OM, Serrano-Villar S, Perez-Brocal V, et al. Analysis of the gut microbiota in alopecia areata: identification of bacterial biomarkers. *J Eur Acad Dermatol Venereol* 2020;34(2):400–405. doi:10.1111/jdv.15885.

[34] Tanoue T, Morita S, Plichta DR, et al. A defined commensal consortium elicits CD8 T cells and anti-cancer immunity. *Nature* 2019;565(7741):600–605. doi:10.1038/s41586-019-0878-z.

[35] Mu Q, Tavella VJ, Luo XM. Role of Lactobacillus reuteri in human health and diseases. *Front Microbiol* 2018;9:757. doi:10.3389/fmicb.2018.00757.

[36] He B, Hoang TK, Wang T, et al. Resetting microbiota by Lactobacillus reuteri inhibits T reg deficiency-induced autoimmunity via adenosine A2A receptors. *J Exp Med* 2017;214(1):107–123. doi:10.1084/jem.20160961.

[37] Hsieh FC, Lan CC, Huang TY, et al. Heat-killed and live Lactobacillus reuteri GMNL-263 exhibit similar effects on improving metabolic functions in high-fat diet-induced obese rats. *Food Funct* 2016;7(5):2374–2388. doi:10.1039/c5fo01396h.

[38] Lawrence T. The nuclear factor NF-kappaB pathway in inflammation. *Cold Spring Harb Perspect Biol* 2009;1(6):a001651. doi:10.1101/cshperspect.a001651.

[39] Wang G, Huang S, Cai S, et al. Lactobacillus reuteri ameliorates intestinal inflammation and modulates gut microbiota and metabolic disorders in dextran sulfate sodium-induced colitis in mice. *Nutrients* 2020;12(8):2298. doi:10.3390/nu12082298.

[40] Luo Z, Chen A, Xie A, et al. Limosilactobacillus reuteri in immunomodulation: molecular mechanisms and potential applications. *Front Immunol* 2023;14:1228754. doi:10.3389/fimmu.2023.1228754.

[41] Abuqwider J, Altamimi M, Mauriello G. Limosilactobacillus reuteri in Health and Disease. *Microorganisms* 2022;10(3):522. doi:10.3390/microorganisms10030522.

[42] Jones SE, Versalovic J. Probiotic Lactobacillus reuteri biofilms produce antimicrobial and anti-inflammatory factors. *BMC Microbiol* 2009;9:35. doi:10.1186/1471-2180-9-35.
[43] Lin YP, Thibodeaux CH, Pena JA, et al. Probiotic Lactobacillus reuteri suppress proinflammatory cytokines via c-Jun. *Inflamm Bowel Dis* 2008;14(8):1068–1083. doi:10.1002/ibd.20448.
[44] Deza G, Ricketti PA, Gimenez-Arnau AM, et al. Emerging biomarkers and therapeutic pipelines for chronic spontaneous urticaria. *J Allergy Clin Immunol Pract* 2018;6(4):1108–1117. doi:10.1016/j.jaip.2018.02.024.
[45] Liu M, Hu R, Guo Y, et al. [Influence of Lactobacillus reuteri SL001 on intestinal microbiota in AD model mice and C57BL/6 mice]. *Sheng Wu Gong Cheng Xue Bao* 2020;36(9):1887–1898. doi:10.13345/j.cjb.200024.
[46] Garg S, Singh TP, Malik RK. In vivo implications of potential probiotic Lactobacillus reuteri LR6 on the gut and immunological parameters as an adjuvant against protein energy malnutrition. *Probiotics Antimicrob Proteins* 2020;12(2):517–534. doi:10.1007/s12602-019-09563-4.
[47] Yang J, Wang C, Liu L, et al. Lactobacillus reuteri KT260178 supplementation reduced morbidity of piglets through its targeted colonization, improvement of cecal microbiota profile, and immune functions. *Probiotics Antimicrob Proteins* 2020;12(1):194–203. doi:10.1007/s12602-019-9514-3.
[48] Liu Y, Tian X, He B, et al. Lactobacillus reuteri DSM 17938 feeding of healthy newborn mice regulates immune responses while modulating gut microbiota and boosting beneficial metabolites. *Am J Physiol Gastrointest Liver Physiol* 2019;317(6):G824–G838. doi:10.1152/ajpgi.00107.2019.
[49] Khmaladze I, Butler E, Fabre S, et al. Lactobacillus reuteri DSM 17938-A comparative study on the effect of probiotics and lysates on human skin. *Exp Dermatol* 2019;28(7):822–828. doi:10.1111/exd.13950.
[50] Zhao Y, Qi C, Li X, et al. Prevention of atopic dermatitis in mice by Lactobacillus reuteri Fn041 through induction of regulatory T cells and modulation of the gut microbiota. *Mol Nutr Food Res* 2022;66(6):e2100699. doi:10.1002/mnfr.202100699.
[51] Fang Z, Pan T, Wang H, et al. Limosilactobacillus reuteri attenuates atopic dermatitis via changes in gut bacteria and indole derivatives from tryptophan metabolism. *Int J Mol Sci* 2022;23(14):7735. doi:10.3390/ijms23147735.
[52] Arshi S, Babaie D, Nabavi M, et al. Circulating level of CD4+ CD25+ FOXP3+ T cells in patients with chronic urticaria. *Int J Dermatol* 2014;53(12):e561–e566. doi:10.1111/ijd.12630.
[53] Chen WC, Chiang BL, Liu HE, et al. Defective functions of circulating CD4+CD25+ and CD4+CD25- T cells in patients with chronic ordinary urticaria. *J Dermatol Sci* 2008;51(2):121–130. doi:10.1016/j.jdermsci.2008.02.012.
[54] Zheng J, Wittouck S, Salvetti E, et al. A taxonomic note on the genus lactobacillus: description of 23 novel genera, emended description of the genus Lactobacillus Beijerinck 1901, and union of lactobacillaceae and leuconostocaceae. *Int J Syst Evol Microbiol* 2020;70(4):2782–2858. doi:10.1099/ijsem.0.004107.